A Recently Evolved Transcriptional Network Controls Biofilm Development in *Candida albicans*

Clarissa J. Nobile,[1,*] Emily P. Fox,[1,2] Jeniel E. Nett,[3] Trevor R. Sorrells,[1,2] Quinn M. Mitrovich,[1,5] Aaron D. Hernday,[1,5] Brian B. Tuch,[1,4] David R. Andes,[3] and Alexander D. Johnson[1]
[1]Department of Microbiology and Immunology
[2]Tetrad Program, Department of Biochemistry and Biophysics
University of California, San Francisco, San Francisco, CA 94102, USA
[3]Department of Medicine, University of Wisconsin, Madison, WI 53706, USA
[4]Present address: Genome Analysis Unit, Amgen, South San Francisco, CA 94080, USA
[5]Present address: Amyris, Emeryville, CA 94608, USA
*Correspondence: clarissa.nobile@ucsf.edu
DOI 10.1016/j.cell.2011.10.048

SUMMARY

A biofilm is an organized, resilient group of microbes in which individual cells acquire properties, such as drug resistance, that are distinct from those observed in suspension cultures. Here, we describe and analyze the transcriptional network controlling biofilm formation in the pathogenic yeast *Candida albicans*, whose biofilms are a major source of medical device-associated infections. We have combined genetic screens, genome-wide approaches, and two in vivo animal models to describe a master circuit controlling biofilm formation, composed of six transcription regulators that form a tightly woven network with ∼1,000 target genes. Evolutionary analysis indicates that the biofilm network has rapidly evolved: genes in the biofilm circuit are significantly weighted toward genes that arose relatively recently with ancient genes being underrepresented. This circuit provides a framework for understanding many aspects of biofilm formation by *C. albicans* in a mammalian host. It also provides insights into how complex cell behaviors can arise from the evolution of transcription circuits.

INTRODUCTION

Biofilms are organized communities of surface-associated micro-organisms embedded in a matrix of extracellular polymers. In this paper, we analyze how *C. albicans*, the predominant fungal pathogen of humans, forms biofilms. Biofilms are a major microbial growth form in natural environments (Kolter and Greenberg, 2006) and a leading cause of persistent human infection (Costerton et al., 1999). These infections are typically seeded from biofilms that form on implanted medical devices, such as intravascular catheters, and become resistant to drug and mechanical treatments (Donlan and Costerton, 2002). The mechanisms behind biofilm development are thus important to our understanding of microbial ecology (because mixed species biofilms are common) as well as infectious disease.

C. albicans biofilm formation can be partitioned into four basic stages, based on studies carried out in vitro (Baillie and Douglas, 1999; Chandra et al., 2001; Douglas, 2003; Hawser and Douglas, 1994; Nobile et al., 2009; Uppuluri et al., 2010a, 2010b). These are: (1) attachment and colonization of yeast-form (nearly spherical) cells to a surface, (2) growth and proliferation of yeast-form cells to allow formation of a basal layer of anchoring microcolonies, (3) growth of pseudohyphae (ellipsoid cells joined end to end) and extensive hyphae (chains of cylindrical cells) concomitant with the production of extracellular matrix material, and (4) dispersal of yeast-form cells from the biofilm to seed new sites. At least some of these features of biofilm formation have also been observed in vivo. For example, *C. albicans* biofilms from denture stomatitis patients confirm the presence of yeast, hyphae, and extracellular matrix (Ramage et al., 2004). Furthermore, biofilm architectures in two animal catheter models and a denture model include numerous yeast cells in the basal region, as well as hyphae and extracellular matrix extending throughout the biofilm (Andes et al., 2004; Nett et al., 2010; Schinabeck et al., 2004).

Here, we combine "classical" genetics, genome-wide approaches, RNA deep sequencing technology, and two in vivo animal models to comprehensively map the transcriptional circuitry controlling biofilm formation in *C. albicans*. The circuit has led to many new predictions about genes involved in biofilm formation, and we have validated a set of these predictions by confirming the roles of several of these genes in biofilm development. The circuit also provides insight into how biofilm formation may have evolved in the *C. albicans* lineage.
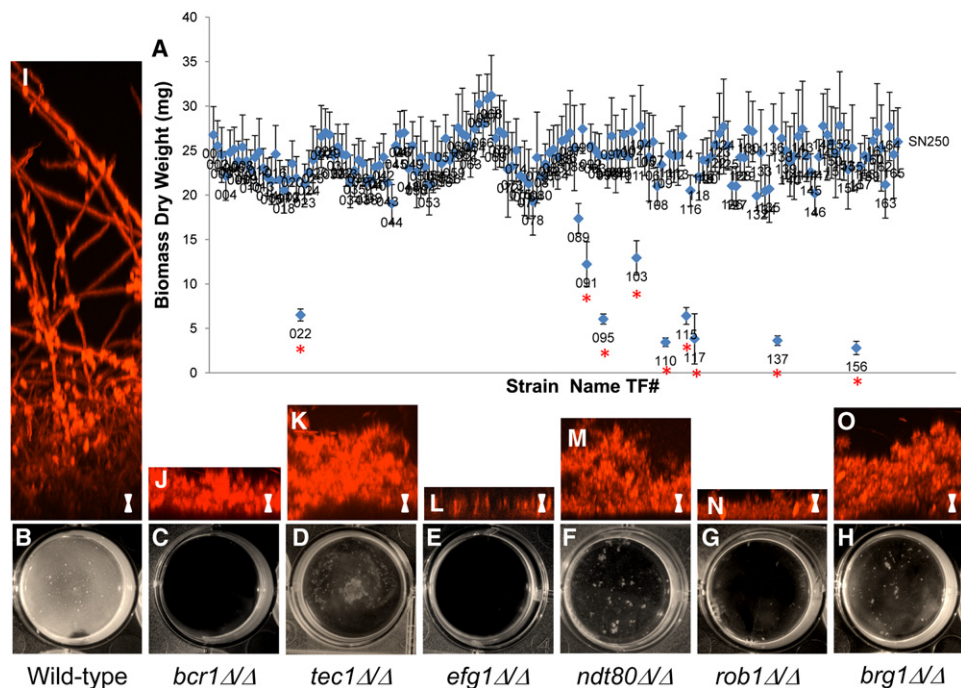
Figure 1. Screening and Characterization of In Vitro Biofilm-Defective Transcription Regulator Mutants

(A) Biofilm biomass (dry weight) determinations of the entire transcription regulator (TR) mutant library (165 strains). The average total biomass ± standard deviation for each TR mutant strain grown under standard biofilm conditions (Experimental Procedures) was calculated from five independent samples of each strain. Statistical significance (p values) was calculated with a Student's one-tailed paired t test and is represented by the red asterisk under the nine regulator strains (TF022, TF091, TF095, TF103, TF110, TF115, TF117, TF137, and TF156) with biomasses significantly deviating (p < 0.0005) from the reference strain (SN250).

(B–O) Phenotypic characterization of the mutants compared to the wild-type.

(B–H) The visual appearance after 48 hr of growth on polystyrene plates.

(I–O) CSLM side view images of the wild-type and six biofilm-defective mutant strains.

Scale bars represent 20 μm. See also Table S1 and Figures S1, S2, and S3.

RESULTS

Identification and Phenotypic Characterization of Biofilm-Defective Transcription Regulator Mutants In Vitro

Transcription regulators (defined here as sequence-specific DNA-binding proteins that regulate transcription) play important roles in the control of many developmental pathways; often, they define a group of coregulated target genes that function together to carry out a specific function in the cell. Hence, transcription regulators represent a powerful entry point to understanding a biological process. Using information on transcription regulators taken from a wide variety of species, we constructed a *C. albicans* library of 165 fully vetted transcription regulator (TR) deletion mutants consisting of two independently constructed mutants for each strain (Homann et al., 2009). This library was screened for biofilm formation on the surface of serum-treated polystyrene plates under a standard set of biofilm-inducing conditions (Nobile et al., 2006a, 2006b; Nobile and Mitchell, 2005). The screening was based on biofilm dry weight biomass, visual, and microscopic (confocal) inspection (Figure 1). The screen revealed nine mutants with deficiencies in forming biofilms (Figure 1A and Table S1 and Figure S2A avail-

able online). Three of these mutants were not analyzed further because they exhibited either general growth defects in suspension cultures or a wide variety of other phenotypes in suspension cultures (Extended Experimental Procedures). The remaining six transcription regulator deletion mutants (*bcr1Δ/Δ*, *tec1Δ/Δ*, *efg1Δ/Δ*, *ndt80Δ/Δ*, *rob1Δ/Δ*, and *brg1Δ/Δ*) have the following characteristics: (1) they were significantly compromised in biofilm formation compared to the wild-type (p < 0.0005) (Figures 1B–1H), (2) they did not exhibit general growth defects, and (3) they did not show extensive phenotypes aside from defects in biofilm formation. Of these six transcription regulators, three are newly identified as biofilm regulators (Ndt80/Orf19.2119, Rob1/Orf19.4998 [named for *r*egulator *o*f *b*iofilms], and Brg1/Orf19.4056 [named for *b*iofilm *reg*ulator]), and three had been previously implicated in biofilm formation (Bcr1 [Nobile and Mitchell, 2005], Tec1 [Nobile and Mitchell, 2005], and Efg1 [Ramage et al., 2002]). The screen was carried out blindly, and our identification of all previously identified regulators serves as an internal control for both the library construction and the screen.

We further characterized the morphology of the six biofilm-defective mutant strains compared to the wild-type by confocal scanning laser microscopy (CSLM), using silicone squares as the substrate (Figures 1I–1O). By CSLM, the wild-type reference

strain formed a biofilm with typical architecture and thickness (Chandra et al., 2001; Douglas, 2003; Nobile and Mitchell, 2005) of ~250 μm in depth, containing both round budding yeast-form cells adjacent to the substrate and hyphal cells extending throughout the biofilm (Figure 1I) (see also Figure S1 for CSLM visualization of each regulator mutant over a time course of biofilm development). In all six mutants, only rudimentary biofilms of ~20–80 μm in depth were formed, although the detailed phenotypes of the mutants differ (Figures 1J–1O and S1). Reintroduction of an ectopic copy of the wild-type allele back into each mutant reversed the biofilm formation defect of each mutant (Figure S2B). Thus, *BCR1*, *TEC1*, *EFG1*, *NDT80*, *ROB1*, and *BRG1* are required for wild-type biofilm formation in vitro.

Because hyphal development is an important step in normal biofilm development, we assessed the ability of our six biofilm-defective transcription regulator mutants to form normal hyphae when they were not in the context of a biofilm. We found that, with the exception of the *efg1Δ/Δ* strain, true hyphae could be detected in the medium surrounding the biofilm (Figure S3A) as well as in suspension cultures using the same medium as that used for biofilm formation (Figure S3B). We also observed hyphal development for all strains except the *efg1Δ/Δ* strain in a variety of suspension culture media, although the fraction of hyphal cells was often reduced relative to the parental strain (Figure S3B). Thus, for all of these mutants (with the possible exception of *efg1Δ/Δ*), the defect in biofilm formation was not due to an intrinsic inability to form hyphae.

Characterization of Biofilm-Defective Transcription Regulator Mutants in Two In Vivo Animal Models

Biofilm formation in vivo is the cause of the majority of new infections in humans, and it is widely appreciated that the conditions for biofilm formation in vivo differ considerably from those in standard in vitro assays (Nett and Andes, 2006). For example, many additional elements are present in vivo, such as liquid flow, host factors, and components of the host immune response. Because biofilm-based catheter infections are a major clinical problem (Kojic and Darouiche, 2004), we used a well-established rat venous catheter model of infection (Andes et al., 2004) to test the six mutants for biofilm formation in vivo. We inoculated the catheters with *C. albicans* cells intraluminally, allowed biofilm formation to proceed for 24 hr, removed the catheters, and visualized the catheter luminal surfaces by scanning electron microscopy (SEM) (Figures 2A–2G and S4A). The wild-type reference strain formed a thick, mature biofilm on the rat catheter, consisting of yeast and hyphal cells and extracellular matrix material (Figure 2A). Of the six transcription regulator mutants, five (*bcr1Δ/Δ*, *tec1Δ/Δ*, *efg1Δ/Δ*, *ndt80Δ/Δ*, and *rob1Δ/Δ*) were unable to form biofilms (Figures 2B–2F); *bcr1Δ/Δ* had been previously shown to be defective in this model (Nobile et al., 2008). The sixth mutant (*brg1Δ/Δ*) formed a thick biofilm consisting of many adherent cells and a large amount of extracellular matrix material (Figure 2G) but appeared morphologically distinct from the reference strain in that considerably fewer hyphae were observed within the biofilm (compare Figures 2A and 2G).

The most common form of oral candidiasis is denture stomatitis, prevalent largely in the elderly population, and affecting up
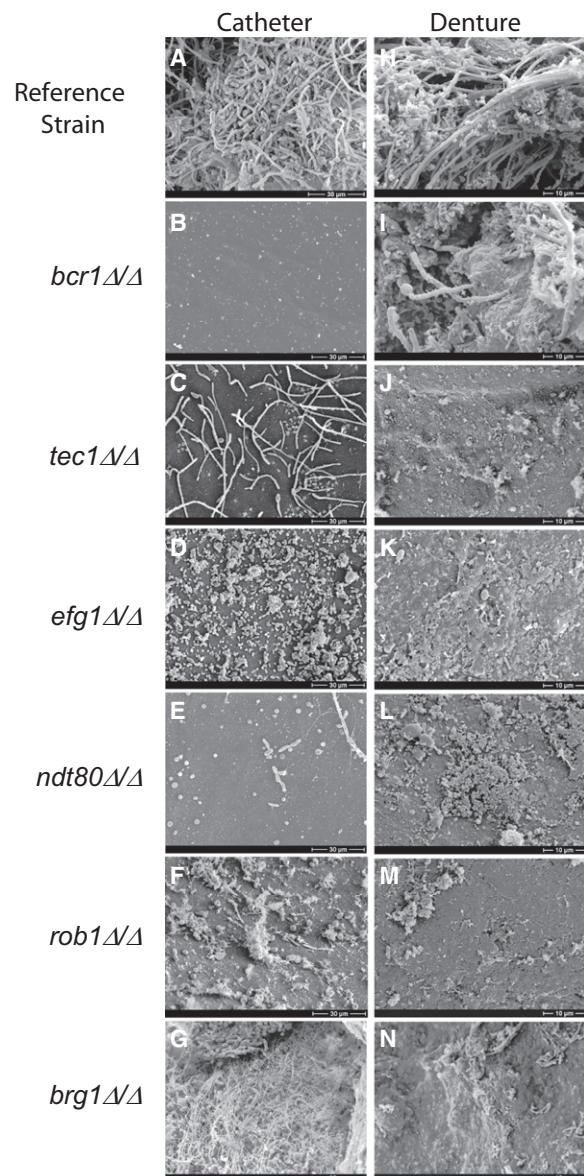
Figure 2. Biofilm Formation in Two In Vivo Rat Models: A Catheter Model and a Denture Model

(A–G) For the catheter model, the wild-type reference strain SN250 (A) and the six transcription regulator mutant strains (panels B–G) were inoculated into rat intravenous catheters; resulting biofilms were visualized after 24 hr of growth by scanning electron microscopy (SEM). SEM catheter images show the catheter luminal surfaces at magnifications of 1,000×.

(H–N) For the denture model, the wild-type reference strain SN425 (H) and the six transcription regulator mutant strains (I–N) were inoculated into rat dentures, and the resulting biofilms were visualized after 24 hr of growth by SEM. SEM denture images show the denture surfaces at magnifications of 2,000×.

See also Figure S4.

to 70% of denture wearers (Webb et al., 1998; Wilson, 1998). Denture stomatitis occurs by biofilm colonization and growth over the surface of a denture, leading to inflammation of the palatal mucosa (Ramage et al., 2004). Because biofilm growth

on dentures represents a completely different host environment from that of an intravenous catheter, we also screened our six biofilm-defective regulator mutants in a recently established in vivo rat denture model, which was developed to mimic and assess *C. albicans* biofilm formation in denture stomatitis (Nett et al., 2010). In particular, this oral model includes host salivary components, host commensal bacteria, salivary flow dynamics, and direct contact between the denture biofilm and the host mucosal surface (Nett and Andes, 2006). We inoculated the rat dentures with *C. albicans* cells, permitted biofilm formation to proceed for 24 hr, removed the dentures, and visualized the denture surfaces by SEM (Figures 2H–2N). The wild-type reference strain formed a thick, mature biofilm on the surface of the rat denture, consisting predominantly of hyphal *C. albicans* cells interspersed with *C. albicans* yeast-form cells, various host commensal oral bacteria, and extracellular matrix material (Figure 2H). In contrast, the genetically matched mutant strains all showed significant defects in biofilm formation. In particular, *tec1Δ/Δ*, *efg1Δ/Δ*, *ndt80Δ/Δ*, *rob1Δ/Δ*, and *brg1Δ/Δ* were severely defective (Figures 2J–2N), whereas the *bcr1Δ/Δ* mutant, which has previously been shown to be defective in this model (Nett et al., 2010), had less pronounced defects than the other five mutants (Figure 2I). We note that extensive bacterial biofilms consisting of both cocci and rods were seen on the dentures of the six *C. albicans* biofilm-defective mutants (Figure S4B), suggesting a competition between biofilm formation by *C. albicans* and biofilm formation by the native bacteria present in the mouth.

In summary, *BCR1*, *TEC1*, *EFG1*, *NDT80*, *ROB1*, and *BRG1* are each required for normal biofilm formation in vivo in both the rat denture and catheter models. The effects of certain deletion mutants (*brg1Δ/Δ* and *bcr1Δ/Δ*) differed to varying degrees between the two models (compare Figures 2G with 2N and 2B with 2I), likely reflecting the influence of the host environment in biofilm formation. The results, taken as a whole, indicate that performing genetic screens and analyzing biofilm formation in vitro is a valid approach to understanding clinically relevant *C. albicans* biofilm formation.

Developing Transcriptional Relationships among Biofilm Regulators

To identify genes directly regulated by Bcr1, Tec1, Efg1, Ndt80, Rob1, and Brg1, we performed full-genome chromatin immunoprecipitation microarray (ChIP-chip) to map the position across the genome to which each of the six transcription regulators is bound during biofilm formation. Based on this analysis (see Extended Experimental Procedures for details, Tables S2A–S2F for a complete list of all significantly bound locations for each regulator, and Data S1 for MochiView image plots of every called significant peak for each regulator), we calculate the following number of intergenic regions bound by each regulator: 211 for Bcr1, 76 for Tec1, 328 for Efg1, 558 for Ndt80, 95 for Rob1, and 283 for Brg1 (Table S2G). 831 intergenic regions are bound by one or more regulators, 350 intergenic regions are bound by two or more, 186 intergenic regions are bound by three or more, 111 intergenic regions are bound by four or more, 55 intergenic regions are bound by five or more, and 18 intergenic regions are bound by all six of the biofilm regulators

(Table S2G). We noticed two unusual characteristics for the intergenic regions bound by the biofilm regulators. First, the average length of intergenic regions bound by the biofilm regulators is more than twice that of the remainder of the genome (1540 bp compared with 693 bp); this trend is true for all six biofilm regulators (Table S4F). Second, binding peaks are distributed throughout the intergenic regions of the regulator-bound target genes rather than being clustered a fixed distance upstream of the transcription start site (Data S2), as is common for many yeast target genes (Lin et al., 2010).

If we convert bound intergenic regions to genes likely to be controlled (for example, a single bound intergenic region between divergently transcribed genes is counted as two genes), our analysis suggests that the network is composed of 1,061 target genes that are bound in their promoter regions by at least one of the six biofilm regulators (Figure 3 and Table S3A). This regulatory network is shown in Figure 3. Based on the ChIP-chip data, the high degree of overlap between target genes among biofilm regulators suggests that the biofilm regulatory network is considerably interwoven; that is, many of the target genes are controlled by more than one regulator.

The results also indicate that the six regulators originally identified in the genetic screen control each other's expression: all six of the regulators bind to the upstream promoter regions of *BCR1* (Figure 4A), *TEC1* (Figure 4B), *EFG1* (Figure 4C), and *BRG1* (Figure 4F); four of the regulators (Tec1, Efg1, Ndt80, and Rob1) bind to the upstream promoter region of *ROB1* (Figure 4E); and two of the regulators (Efg1 and Ndt80) bind to the upstream promoter region of *NDT80* (Figure 4D).

De Novo Motif Finding for the Six Master Biofilm Regulators

A test of the self-consistency of ChIP-chip data is the nonrandom occurrence of *cis*-regulatory sequences (motifs). Based on several hundred significant binding events from our ChIP-chip data, we were able to identify statistically significant motifs for all six of the biofilm regulators (Figure 4G, Data S2, and Tables S2H–S2M). This motif generation was based solely on the ChIP-chip data and did not incorporate data from any other experiment or from any other species. We note that the motif generated for Ndt80 (TTACACAAAA) is very similar to the reported binding motif for its homolog, Ndt80, in *S. cerevisiae* (GMCACAAAA) (Zhu et al., 2009). The motif for Tec1 (RCATTCY) is identical to that determined for its homolog, Tec1, in *S. cerevisiae* (Harbison et al., 2004; Madhani and Fink, 1997). (This Tec1 motif, generated from 107 bound intergenic regions, does not closely resemble the Tec1 motif recently reported in the white-specific pheromone response element [WPRE] [AAAAAAAAAAGAAAG] in *C. albicans*, which was generated from a much smaller set of data [Sahni et al., 2010].) Finally, the Efg1 motif derived from our ChIP-chip data (RTGCATRW) closely resembles the TGCAGNNA consensus sequence of the *S. cerevisiae* ortholog, Sok2 (Harbison et al., 2004). Thus, for three of the biofilm regulators, the motifs developed from our *C. albicans* ChIP-chip data can be independently verified by their similarities to the motifs recognized by their *S. cerevisiae* orthologs. This analysis provides independent support for both the motif analysis and for the validity of the full-genome ChIP data. For the other three regulators, we were able
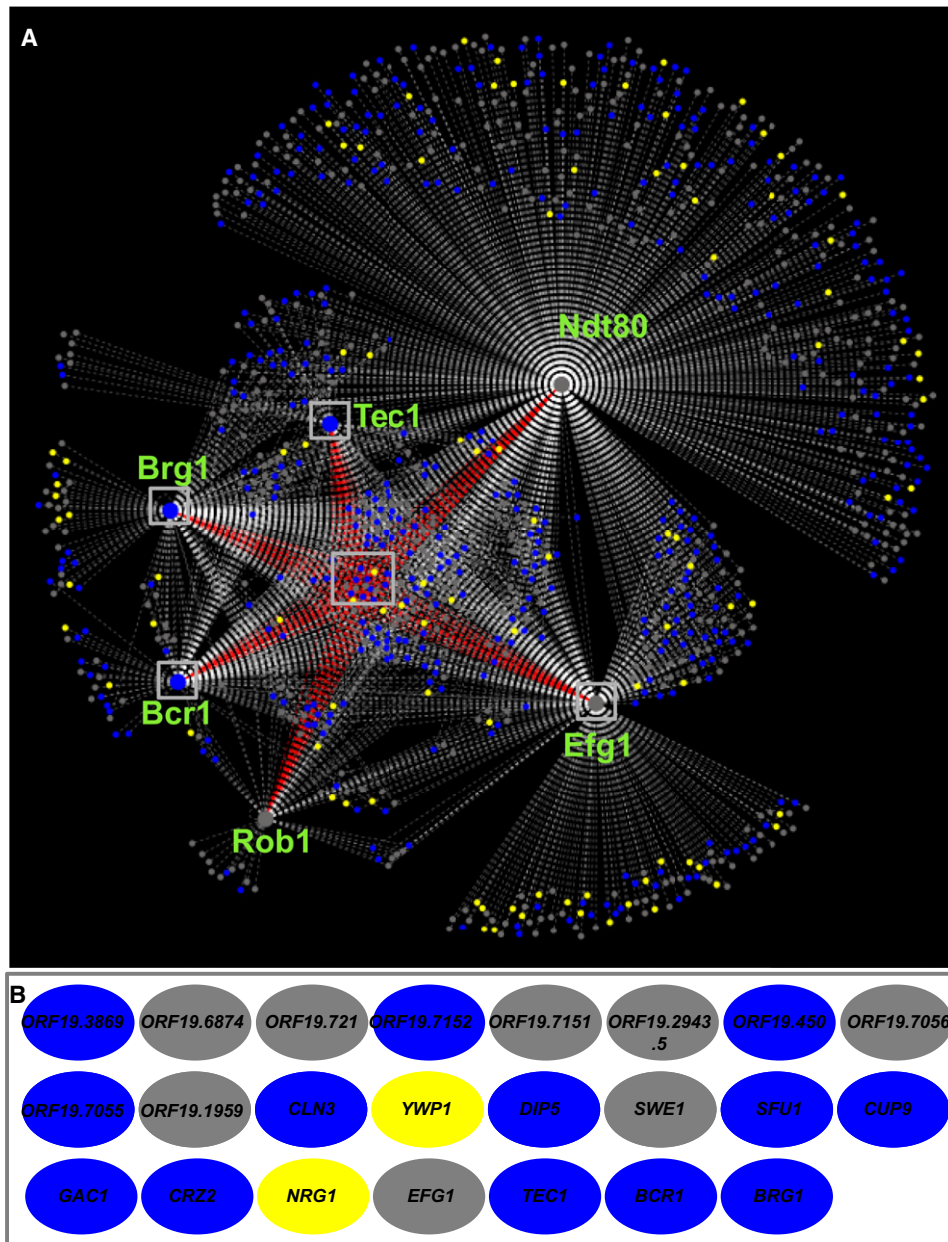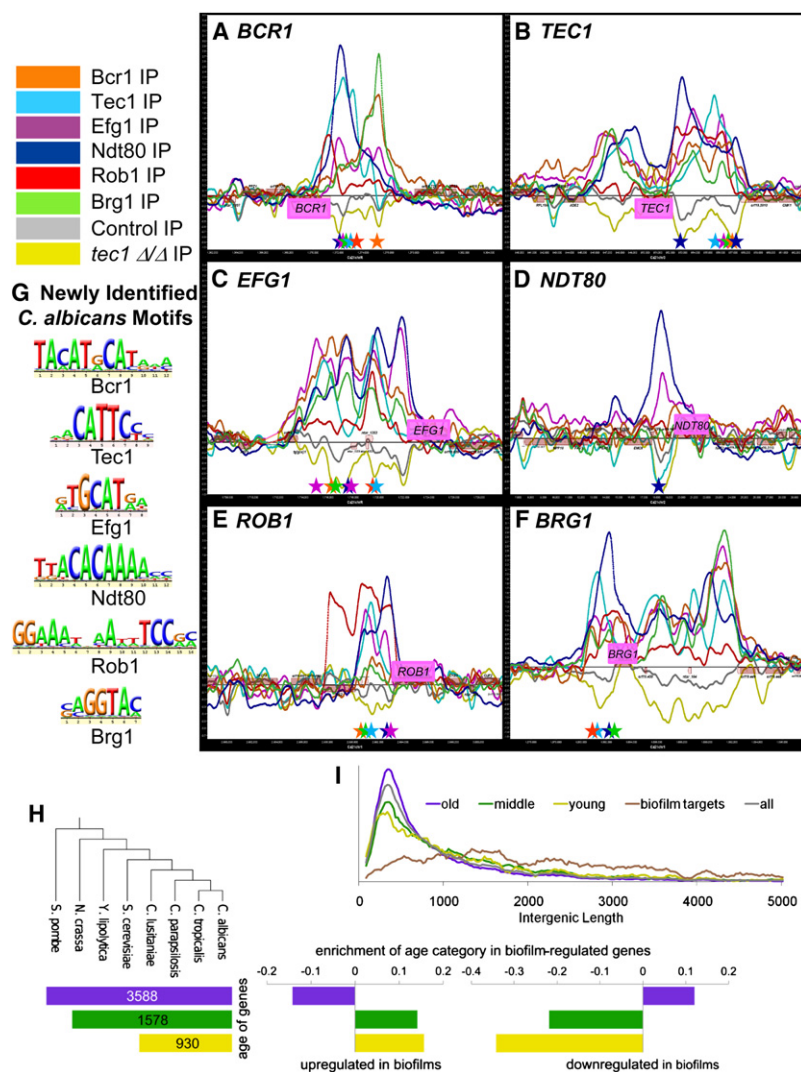
Figure 3. The Biofilm Regulatory Network

(A and B) The six master biofilm regulators are represented by the six large circular hubs. Smaller circles represent target genes, which are connected to their respective regulators by dashed lines, indicating a direct interaction as determined by genome-wide ChIP-chip. Genes that are differentially regulated as determined by expression data (using a 2-fold cutoff) in biofilm compared to planktonic cells are shown in blue for those genes upregulated in biofilms, in yellow for those downregulated, and in gray for those with no change. Gray boxes are drawn around the 23 target genes bound by all six regulators and are connected to their respective regulators by red dashed lines (A). The identity of these 23 genes are indicated as the colored ovals in (B) (blue ovals are genes that are upregulated, yellow ovals are genes that are downregulated, and gray ovals are genes with no change in biofilm compared to planktonic cells). Overall, 23 genes are bound by all six, 77 are bound by five or more, 165 are bound by four or more, 265 are bound by three or more, and 458 are bound by two or more of the biofilm regulators. See also Table S3A.

to determine statistically significant motifs, but we were not able to independently verify them by comparison with *S. cerevisiae* because either the orthology relationships are uncertain (Rob1 and Brg1) or the orthologous *S. cerevisiae* regulator has not been characterized (Bcr1).

Exploring the Transcriptional Patterns of Biofilms

Although the ChIP-chip experiments reveal the genomic positions where each regulator binds, they do not indicate whether these binding events are associated with differences in gene transcription. We first consider control of the regulators

A *BCR1*

B *TEC1*

C *EFG1*

D *NDT80*

E *ROB1*

F *BRG1*

Bcr1 IP
Tec1 IP
Efg1 IP
Ndt80 IP
Rob1 IP
Brg1 IP
Control IP
tec1 Δ/Δ IP

G Newly Identified *C. albicans* Motifs

Bcr1

Tec1

Efg1

Ndt80

Rob1

Brg1

H

S. pombe
N. crassa
Y. lipolytica
S. cerevisiae
C. lusitaniae
C. parapsilosis
C. tropicalis
C. albicans

3588
1578
930

age of genes

enrichment of age category in biofilm-regulated genes

upregulated in biofilms

downregulated in biofilms

I

old — middle — young — biofilm targets — all

Intergenic Length

Figure 4. Chromatin Immunoprecipitation Mapping and Motif Identification of the Six Master Biofilm Regulators and Evolutionary Analysis of the Biofilm Target Genes

(A–G) All six regulators bind to each another's upstream promoter regions (A–F). Immunoprecipitation (IP) binding data for Bcr1-Myc (orange line), Tec1-custom antibody (light blue line), Efg1-Myc (magenta line), Ndt80-Myc (dark blue line), Rob1-Myc (red line), Brg1-Myc (green line), untagged wild-type/control IP (gray line), and *tec1Δ/Δ* (yellow line) strains are shown. The ChIP-chip microarray binding data was mapped and plotted onto the chromosomes containing *BCR1* (A), *TEC1* (B), *EFG1* (C), *NDT80* (D), *ROB1* (E), and *BRG1* (F) using MochiView. The promoters of these genes show significant peak enrichments for the binding of the indicated biofilm regulators. The x axis represents ORF chromosomal locations. The y axis gives the Agilent normalized enrichment value (log2) postsmoothing for the binding of each regulator. Genes (pink boxes) plotted above the bold line read in the sense direction; genes plotted below the bold line read in the antisense direction. Using de novo motif finding based on our ChIP-chip data, we identified significantly enriched core binding motifs for all six biofilm regulators (G). Motifs were identified using MochiView and independently verified using MEME, and motif graphics were generated with MochiView. Colored stars corresponding to the colors of the regulators indicate the location of strong instances of the indicated biofilm regulator motifs under the enrichment peaks in A–F.

(H) The evolutionary age of target genes in the biofilm network. Genes were divided into three categories based on when they arose during evolution, with the numbers in each bar giving the number of *C. albicans* genes that fall into that age category (based on the union of RNA-seq and microarray data sets for biofilm versus planktonic cells). The enrichment of each age category in biofilm-regulated genes is $\log_{10}$ of the observed divided by the expected (for all age categories, $p < 1.23 \times 10^{-9}$).

(I) A histogram of the length of the intergenic regions between tandem and divergent gene pairs targeted by the biofilm regulators. Each category was normalized to the total number of intergenic regions in that category.

See also Data S1 and S2 and Tables S2, S3, S4, and S5.

themselves, as they are all bound by one or more of the other regulators. We deleted each regulator and measured the mRNA levels of the other five (Figure S7A). This analysis revealed that each regulator positively regulates each of the other regulators. We also examined the effect of each regulator on its own synthesis by fusing its upstream region to an mCherry reporter and measuring levels of the reporter in the absence and presence of the regulator (Figure S7B). In all cases, a given regulator activates its own synthesis. Thus, the connections among the six biofilm regulators are primarily, if not exclusively, positive.

To assess the relationship of regulator binding and transcription across the entire circuit, we performed both RNA-seq and gene expression microarray analyses of cells grown in biofilm and planktonic conditions. From our RNA-seq data, we generated 46 million mappable strand-specific sequence reads, expanding our previous gene annotation (Tuch et al., 2010) by identifying 622 "novel transcriptionally active regions" (nTARs) and 161 nTARs that overlap, at least partially, transcribed regions identified in other recent genome-wide experimental annotations

(Bruno et al., 2010; Sellam et al., 2010) (Table S4A). We know from previous work that nTARs identified by RNA-seq include both noncoding RNAs (Mitrovich et al., 2010) and transcripts that encode for proteins too short to have been identified in previous genome annotations (Tuch et al., 2010).

We used our RNA-seq data in addition to our gene expression microarray data to obtain a complete set of genes (coding and noncoding) differentially expressed between planktonic and biofilm conditions (Table S4). Combining the RNA-seq and microarray data, we find 1,599 genes upregulated and 636 genes downregulated at least 2-fold in biofilm compared to planktonic cells (Tables S4B and S4C, respectively). By analyzing the overlap between our ChIP-chip data and our gene expression data (Table S5), we find a strong correlation between transcription regulator binding and differential gene expression. For example, if we consider regions bound by at least four transcription regulators, ∼60% of these regions are associated with differentially expressed transcripts. This is significantly greater than that expected by chance ($p < 0.0001$) and suggests, at least broadly,

that binding of the regulators is associated with differential transcription in biofilm versus planktonic cultures. For the correlation between the binding of a given single transcription regulator and differential gene expression, we find a range of 38%–56%, comparable to or greater than the associations documented for other *C. albicans* transcription regulators (Askew et al., 2011; Lavoie et al., 2010; Nobile et al., 2009; Sellam et al., 2009; Tuch et al., 2010).

We examined the evolutionary history of genes that are differentially regulated under biofilm conditions. To do this, we categorized each *C. albicans* gene into an age group based on orthology mappings across the Ascomycota, a large group of yeasts that includes both *C. albicans* and *S. cerevisiae* (Wapinski et al., 2007) (Extended Experimental Procedures). Gene ages were defined using orthology assignments from The Fungal Orthogroups Repository (http://www.broad.mit.edu/regev/orthogroups/). The oldest genes are present in distantly related yeast clades, whereas the youngest are found only in *C. albicans*. Young genes can arise in several ways, including relatively rapid mutation that obscures the relation to an ancient gene, horizontal gene transfer, and de novo gene formation (Long et al., 2003). We found that genes upregulated in biofilms are enriched for young and middle-aged genes and are depleted in old genes. The opposite trend was observed for genes that are downregulated in biofilms (Figure 4H). Genes that were not differentially expressed were not strongly enriched for any age category (Table S4E). Young genes typically show longer intergenic regions than old genes (Sugino and Innan, 2011), and this trend may help to explain the unusually long intergenic regions of biofilm circuit genes. However, biofilm genes exhibited significantly longer intergenic regions even when compared to other young genes ($p < 2.2 \times 10^{-16}$) (Figure 4I).

Identifying Functionally Relevant Target Genes of the Master Biofilm Network

To understand the connections between the six regulators and biofilm development, we performed gene expression microarray experiments of all six regulator mutants compared to a reference strain under biofilm-forming conditions. In interpreting this data, it is important to keep in mind that the mutant strains do not form mature biofilms under these conditions, so many of the transcriptional effects may be indirect consequences of defective biofilms. Consistent with this idea, the transcriptional responses to deletion of each of the biofilm transcription regulators tended to encompass a relatively large set of genes (Table S3A). For example, we found 234 genes that were downregulated and 173 genes that were upregulated in the *bcr1Δ/Δ* mutant relative to the isogenic parent (threshold of [log₂ > 0.58 and log₂ < −0.58]) (Table S3C). Of these genes, Bcr1 binds directly to the promoters of 46 (11%) of them, a number that is significantly higher than that predicted by chance (p = 0.0002). Nonetheless, the results indicate that most of the effects of deleting Bcr1 are indirect. Of the genes directly bound by Bcr1, half were downregulated and half were upregulated in the *bcr1Δ/Δ* mutant, indicating that Bcr1 can act as both an activator and repressor of its direct target genes. Similar analysis (Table S3C and Extended Experimental Procedures) indicates that Efg1, Ndt80, Rob1, and Brg1 are all both activators and repressors of

their biofilm-relevant direct target genes and that Tec1 is primarily an activator of its biofilm-relevant direct target genes.

From these large data sets, we attempted to identify a set of target genes that might be expected to have important roles in biofilm formation. Using hierarchical cluster analysis to characterize genes with similar patterns of expression in each of the six biofilm regulator mutants compared to a reference strain under biofilm conditions, we found 19 target genes that were differentially regulated in all six data sets (threshold of [log₂ > 0.58, and log₂ < −0.58]) (Figure 5A and Table S3A). Eight of these target genes (*ORF19.3337*, *ALS1*, *TPO4*, *ORF19.4000*, *EHT1*, *HYR1*, *HWP1*, and *CAN2*) were expressed at lower levels in all six of the biofilm regulator mutants compared to the reference strain (Figure 5A); seven of these genes were also expressed at higher levels in biofilm compared to planktonic wild-type cells (Table S3A). Additionally, all of these eight target genes were bound in their upstream promoter regions by at least one of the six biofilm regulators; most were bound by multiple regulators (Figures 5B–5I).

Further analysis of the regulation of these eight target genes helps to reconcile their expression patterns with the chromatin IP results. As indicated in Figure S5, the transcriptional effects of deleting each one of the six regulators can be accounted for by: (1) direct binding and transcriptional activation by that regulator on the target gene and/or (2) direct binding and activation of a different regulator that, in turn, binds directly to and activates the target gene (Figure S5). This "hierarchical cascade" between the biofilm regulators and target genes, applied more broadly, can explain much of the expression data (Figure S5, Tables S3A and S3C, and Extended Experimental Procedures).

To determine whether the eight target genes identified by this analysis affected biofilm formation, we constructed homozygous deletion strains for each of the eight target genes. We observed significant biofilm defects for *als1Δ/Δ* (p = 0.01), *hwp1Δ/Δ* (p = 0.01), and *can2Δ/Δ* (p = 0.003) mutant strains compared to the reference strain, with the *can2Δ/Δ* strain the most defective (Figure 6A). Although all three of these mutants were capable of forming partial biofilms, these biofilms were less stable than those of the wild-type and often detached from the substrate; partial biofilm defects have been previously reported for *als1Δ/Δ* and *hwp1Δ/Δ* mutant strains (Nobile et al., 2006a, 2006b; Nobile et al., 2008), whereas *can2Δ/Δ* is new to this study. The other five knockout strains did not show any obvious biofilm defects under the conditions tested, and we hypothesized that their roles may be masked by genetic redundancy. To explore this idea, we created ectopic expression strains in which each of the eight target genes was ectopically expressed in strains in which each transcription regulator was deleted. In other words, in a grid of 6 × 8 = 48 constructed strains, we determined whether ectopic expression of the target genes could suppress the defect of the original transcription regulator deletion. Overexpression of several of the candidate target genes was able to significantly rescue biofilm formation to varying degrees depending on the target gene mutant background combination (p < 0.0005) (Figure 6B; see Figure S6 for CSLM images of the rescued biofilms). For example, overexpression of *ORF19.4000*, *CAN2*, or *EHT1* in the *bcr1Δ/Δ* mutant strain background was able to rescue biofilm formation to near wild-type
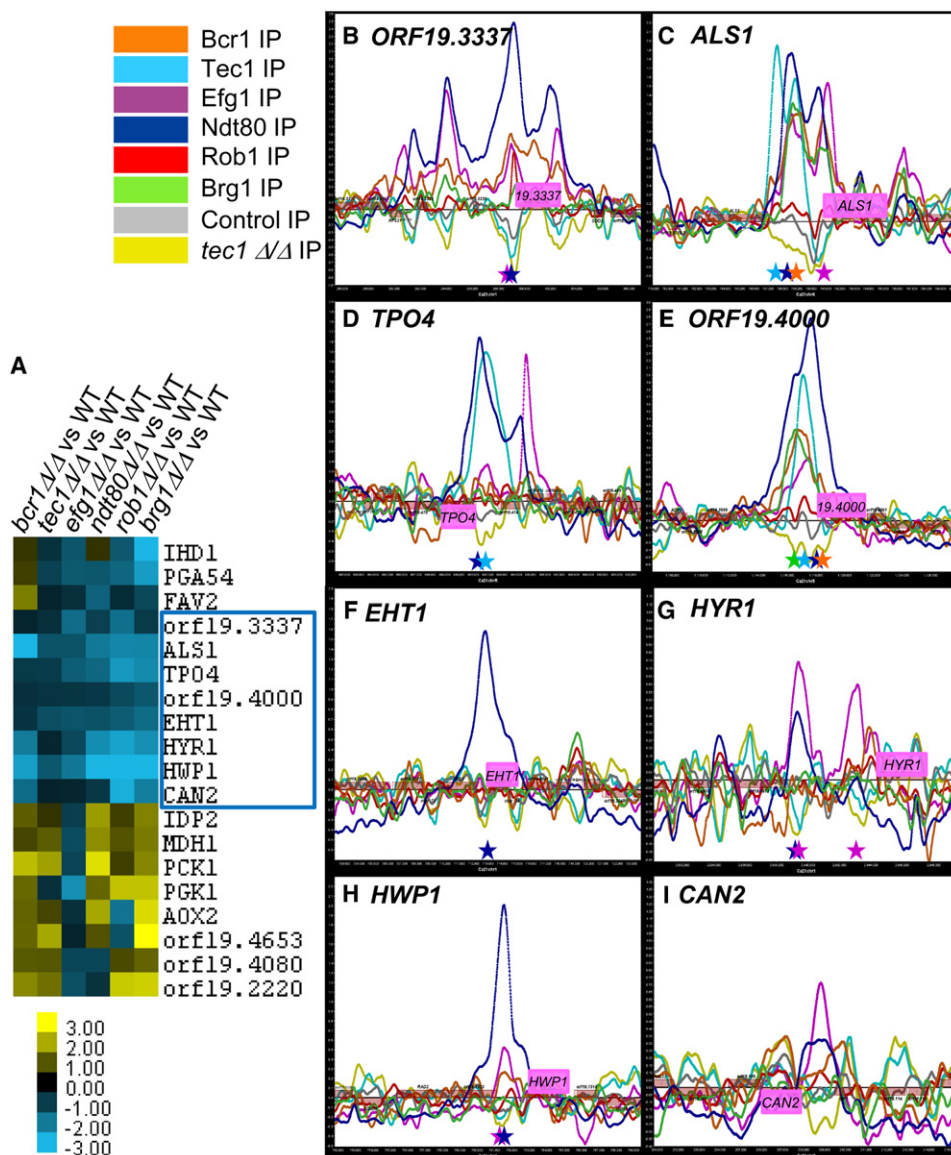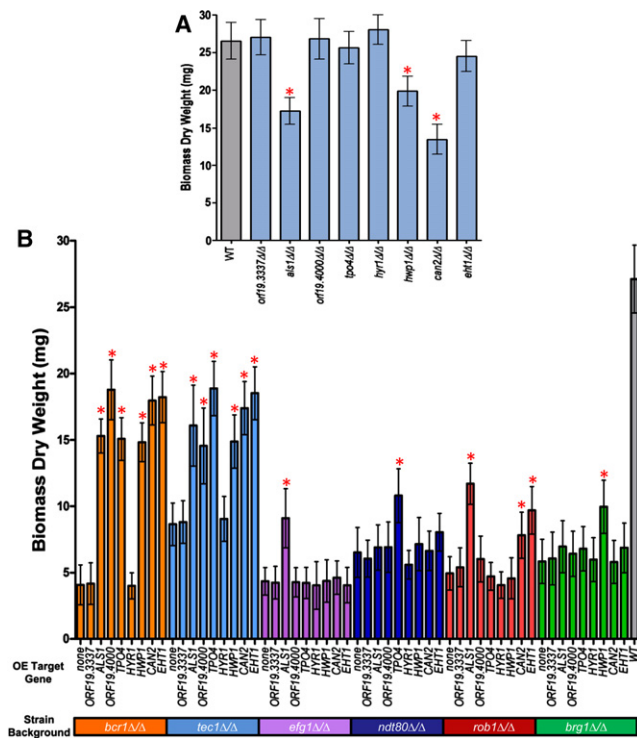
Figure 5. Core Candidate Biofilm Target Genes

(A) Using hierarchical cluster analysis of our gene expression microarray data, we identified a set of 19 candidate target genes (*IHD1*, *PGA54*, *FAV2*, *ORF19.3337*, *ALS1*, *TPO4*, *ORF19.4000*, *EHT1*, *HYR1*, *HWP1*, *CAN2/ORF19.111*, *IDP2*, *MDH1*, *PCK1*, *PGK1*, *AOX2*, *ORF19.4653*, *ORF19.4080*, and *ORF19.*2220) that were differentially regulated (log$_2$ > 0.58, and log$_2$ < −0.58) in all gene expression array experiments that compared each biofilm regulator mutant to a reference strain under biofilm conditions (A). Eight of these targets were differentially regulated in the same direction (all down in the mutants) and were chosen for further functional analyses (A, as indicated by the blue square).

(B–I) ChIP-chip enrichment data for the binding of the six biofilm regulators in the promoters of these eight candidate target genes. IP binding data for Bcr1-Myc (orange line), Tec1 custom antibody (light blue line), Efg1-Myc (magenta line), Ndt80-Myc (dark blue line), Rob1-Myc (red line), Brg1-Myc (green line), untagged wild-type/control IP (gray line), and *tec1Δ/Δ* (yellow line) strains are shown. The ChIP-chip microarray binding data were mapped and plotted onto the chromosomes containing *ORF19.3337* (B), *ALS1* (C), *TPO4* (D), *ORF19.4000* (E), *EHT1* (F), *HYR1* (G), *HWP1* (H), and *CAN2* (I) using MochiView. The promoters of these genes show significant peak enrichments for the binding of the indicated biofilm regulators: *ORF19.3337* by Bcr1, Efg1, Ndt80, and Rob1 (B); *ALS1* by Bcr1, Tec1, Efg1, Ndt80, and Brg1 (C); *TPO4* by Tec1 and Ndt80 (D); *ORF19.4000* by Bcr1, Tec1, Efg1, Ndt80, and Brg1 (E); *EHT1* by Ndt80 (F); *HYR1* by Efg1 (G); *HWP1* by Ndt80 (H); and *CAN2* by Efg1 (I). The x axis represents ORF chromosomal locations. The y axis is the Agilent normalized enrichment value (log2) postsmoothing for the binding of each regulator. Genes (pink boxes) plotted above the bold line read in the sense direction; genes plotted below the bold line read in the antisense direction. Colored stars corresponding to the colors of the regulators indicate the location of strong instances of the indicated biofilm regulator motifs under the enrichment peaks.

See also Figure S5 and Table S3.

Figure 6. Functionally Relevant Biofilm Target Genes
(A and B) Biofilm biomass (dry weight) determinations were measured for the eight core candidate biofilm target gene deletion mutants (A) and the strains in which each of the eight target genes was ectopically expressed in the background of each regulator mutant (B). The average total biomass ± standard deviation for each strain grown under standard biofilm conditions was calculated from five independent samples of each strain. Statistical significance (p values) was calculated with a Student's one-tailed paired t test and is represented by the red asterisks above the strains with biomasses significantly deviating (p < 0.0005) from either the reference strain (WT) for (A) or the corresponding mutant strain for (B). See also Figure S6 and Table S3.

levels of biomass (although the biofilms are fragile) (Figure 6B and Figure S6), implicating these genes in biofilm formation. Taken as a whole, our data suggest that six of the original set of eight candidate target genes have direct roles in biofilm formation. Of course, there are more than 1,000 additional target genes, and their analysis is a future challenge.

DISCUSSION

A Master Transcription Network Controlling Biofilm Formation in *C. albicans*

We have described a master circuit of six transcription regulators that controls biofilm formation by *C. albicans* in vitro and in two different animal models. *C. albicans* biofilms are an organized structure of three types of cells (yeast, pseudohyphae, and hyphae) enclosed in an extracellular matrix. The transcription regulators form an elaborate, interconnected transcriptional network: each regulator controls the other five, and most target genes are controlled by more than one master regulator (Figure 3). The circuit appears to be based largely, if not exclusively, on positive regulation (Figures 7, S7A, and S7B). Taking into
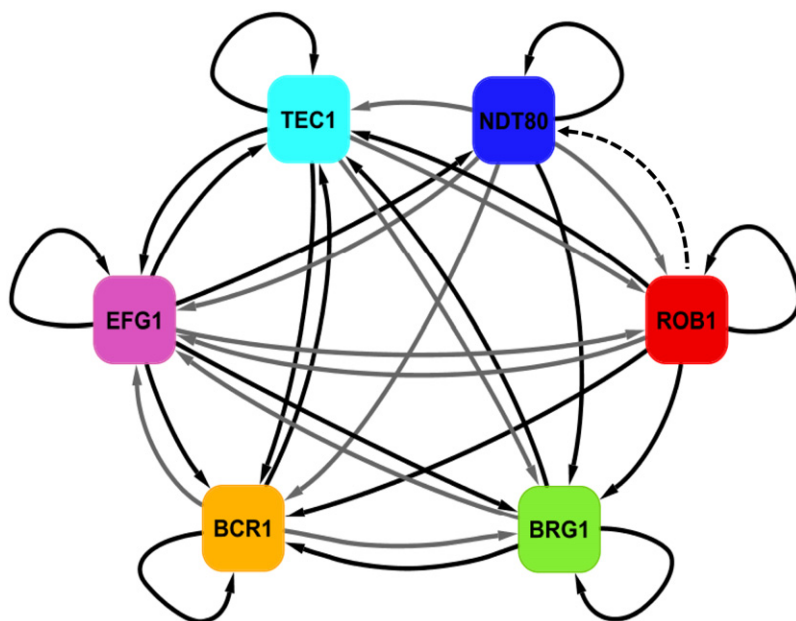
consideration all of the target genes of the six regulators, the biofilm network comprises about 15% of the genes in the genome.

Circuit Complexity

Although the circuit is large and complex (~1,000 genes and twice that many connections), this level of complexity is not without precedent. For example, circuits that control osmotic stress and pseudohyphal growth pathways of *S. cerevisiae* (Borneman et al., 2006; Ni et al., 2009), competence and spore formation in *Bacillus subtilis* (de Hoon et al., 2010; Hamoen et al., 2003; Losick and Stragier, 1992; Süel et al., 2006), the hematopoietic and embryonic stem cell differentiation pathways of mammals (Wilson et al., 2010; Young, 2011), and the regulation of circadian clock rhythms in *Arabidopsis thaliana* (Alabadí et al., 2001; Locke et al., 2005) show certain similarities: they all consist of a core group of master transcription regulators that control each other and—working together—control a large set of additional target genes.

Several possibilities might account for the complexity of the biofilm network. The regulators we have described can orchestrate biofilm formation in two very different niches of the human host: the bloodstream and the oral cavity. It seems likely that the same circuit also controls biofilm formation in other host niches (for example, in the vagina and gastrointestinal tract). Thus, the biofilm circuit responds to many environmental conditions, such as temperature, nutrient availability, flow rate, surface type, other microbial species, and components of the host immune system. One possibility is that the complex circuit that we have described can integrate a wide range of environmental cues to produce a stereotyped morphological and functional output under many different conditions. Consistent with this idea is the finding that one regulator (Bcr1) plays an important role in biofilm formation in the catheter model but has a less pronounced role in the denture model, whereas another regulator (Brg1) shows the opposite behavior. It is also possible that the complex structure of the network (consisting of many direct and indirect feedback loops, many feed-forward loops, and highly overlapping regulons) is responsible for a form of cell memory that acts over generations to ensure coordinated cooperation among cells in maintaining the biofilm state. A third possibility, as has been suggested for ribosomal protein gene regulation (Müller and Stelling, 2009), is that the more complex the regulatory architecture of a network, the more precisely the dynamics of gene expression can be regulated.

A consideration of the evolution of the biofilm network might also help to explain why it differs structurally from simple regulatory schemes. Incorporation of genes one at a time into a network requires a gain of a binding site upstream of each gene; however, bringing a regulatory protein gene into a network instantly incorporates all of that regulator's targets into the network. Thus, the interconnectedness of the biofilm network may reflect the ease by which many genes can be simultaneously incorporated into an existing circuit. Finally, it is formally possible that the complexity per se of a transcriptional network is not, in itself, adaptive; rather, some aspects of the network complexity could simply be the result of neutral (nonadaptive) evolution (Fernández and Lynch, 2011).

Figure 7. Regulatory Network Model for Biofilm Formation

The biofilm network model based on our ChIP-chip and expression data is shown. Solid arrows indicate direct binding interactions determined by our ChIP-chip analysis. Solid black arrows indicate experimentally validated regulatory interactions (as determined by expression profiling data and validated by qPCR) in addition to direct binding interactions (as determined by ChIP-chip data), and solid gray arrows indicate direct binding interactions only. The dashed black arrow indicates an indirect regulatory interaction only. See also Table S3 and Figure S7.

Evolutionary Conservation of the Biofilm Network

Only a few of the many (probably more than a million) fungal species can proliferate and cause disease in humans. These pathogenic species are widely distributed over the fungal lineage, indicating that survival in a human host probably evolved independently multiple times. Although many fungal species can form aggregates (flocs, mats, biofilms, etc.), it seems likely that *C. albicans* is one of very few fungal species that can efficiently form biofilms in a healthy mammalian host. How then did the biofilm circuit evolve in the *C. albicans* lineage?

Several lines of evidence suggest that the biofilm network in *C. albicans* has undergone extensive evolutionary change relatively recently. First, as described in the Results, "young" genes are enriched in the biofilm circuit and "old" genes are underrepresented (Figure 4H). For example, ~120 *C. albicans* genes appear to have arisen (or at least have changed extensively) after the common ancestor of *C. albicans* and *Candida tropicalis* (a closely related species), and one-third of these are part of the biofilm circuit. Second, if we map (when possible) the *C. albicans* biofilm circuit target genes to other species, we find the motifs of two of the master regulatory proteins (Ndt80 and Efg1) only sporadically enriched in these genes (Figure S7C). Thus, the regulator-target gene connections are not strongly conserved outside of *C. albicans* itself. (This analysis could not be meaningfully performed for the other regulators due to a lack of predictive power of their motifs [see Extended Experimental Procedures]). Third, the intergenic regions targeted by biofilm regulators are much longer than average (Figure 4I), possibly providing a larger mutational target for the gain of binding sites. In combination with short motifs, this may help to explain how new genes have quickly become incorporated into the network. Finally, as we discuss in greater detail below, the functions of the master transcription regulators in *C. albicans*

have diverged significantly from their "assignments" in *S. cerevisiae*. Our data and analyses suggest that the biofilm networks of other CTG clade species (species that translate the CUG codon into serine instead of the conventional leucine, e.g., *C. tropicalis*, *Candida parapsilosis*, *Lodderomyces elongisporus*, *Debaryomyces hansenii*, *Candida guiermondii*, and *Candida lusitaniae*) will likely be comprised of different transcription regulators and/or different target genes, or both.

Evolutionary Reassignment of Transcription Regulators

A direct comparison between *C. albicans* and its nonpathogenic relative *S. cerevisiae* provides additional insight into how the biofilm network evolved. We can ask, for example, whether the six master transcription regulators of biofilm formation in *C. albicans* have clear orthologs in *S. cerevisiae* and, if so, what processes they regulate in *S. cerevisiae*. To explore orthology relationships for the master biofilm regulators, we used SYNERGY and INPARANOID mappings, in addition to hand annotation using constructed gene trees. Details are given in Extended Experimental Procedures.

Overall, this analysis indicates that the biofilm circuit consists of two regulators (Tec1 and Efg1) whose broad function—regulation of cell morphology—is deeply conserved in the fungal lineage. However, the set of target genes controlled by these regulators differs significantly between *S. cerevisiae* and *C. albicans* (Extended Experimental Procedures). A third regulator (Ndt80) is deeply conserved in the fungal lineage, but its function appears completely different between *S. cerevisiae* and *C. albicans.* In the former, it regulates meiosis (Hepworth et al., 1998) and, in the latter, biofilm formation. Two regulators (Rob1 and Brg1) are detectable only in species closely related to *C. albicans*, and the sixth biofilm regulator (Bcr1) has orthologs in *S. cerevisiae*, but they have not been characterized. Given that the DNA binding specificity of Tec1, Efg1, and Ndt80 is strongly conserved, extensive gains and losses of *cis*-regulatory sequence must be responsible, at least in part, for the evolution of the biofilm circuit in the *C. albicans* lineage. The Rob1 and Brg1 proteins appear to have undergone extensive changes in the *C. albicans* lineage such that their direct connection to the ancestor of *C. albicans* and *S. cerevisiae* (if any) has been

obscured. Thus, it seems likely that extensive changes in both regulators and *cis*-regulatory sequences were necessary for the evolution of the modern *C. albicans* biofilm circuit. These considerations, in combination with our analysis of "young" versus "old" genes, indicate that the *C. albicans* biofilm circuit evolved relatively recently, and we suggest that this development had an important role in the ability of *C. albicans* to adapt to its human host.

EXPERIMENTAL PROCEDURES

Strain Construction
Primer sequences (Table S7) and *C. albicans* strains (Table S6) are described in the Extended Experimental Procedures; strains were constructed in isogenic backgrounds.

In Vitro Biofilm Growth, Confocal Microscopy, and Biomass Determination
In vitro biofilm growth assays were carried out in Spider medium as described in detail in the Extended Experimental Procedures. The average total biomass for each strain was calculated from five independent samples. Statistical significance (p values) was calculated with a Student's one-tailed paired t test.

In Vivo Rat Catheter Biofilm Model
A rat central-venous catheter infection model (Andes et al., 2004) was used for in vivo biofilm modeling to mimic human catheter infections, as described in detail in the Extended Experimental Procedures. Catheters were removed after 24 hr of *C. albicans* infection to assay biofilm development on the intraluminal surface by scanning electron microscopy (SEM).

In Vivo Rat Denture Biofilm Model
A rat denture stomatitis infection model (Nett et al., 2010) was used for in vivo biofilm modeling to mimic human denture infections, as described in Nett et al. (2010), with certain modifications described in the Extended Experimental Procedures. Dentures were removed after 24 hr post *C. albicans* infection to assay biofilm development on the denture surface by SEM.

RNA Sample Preparation and Extraction
Details on growth, cell harvesting, RNA extraction, and treatment of biofilm and planktonic cells used for gene expression microarray and RNA-seq analysis are described in the Extended Experimental Procedures.

Gene Expression Microarray Design and Analysis
We used custom-designed *C. albicans* oligonucleotide microarrays (AMADID #020166) and a cutoff of 2-fold in both directions ($\log_2 > 1.0$ and $\log_2 < 1.0$) for the differential expression of biofilm versus planktonic cells and 1.5-fold in both directions ($\log_2 > 0.58$ and $\log_2 < -0.58$) for the differential expression of mutant over wild-type (Extended Experimental Procedures and Table S3A).

Full-Genome Chromatin Immunoprecipitation Tiling Microarray
Each transcription regulator was tagged with a Myc tag at the C- or N-terminal end of the protein in a wild-type reference strain background. (In the case of Tec1, tagging the protein at either the C- or N- terminal end interfered with the protein's activity, and we used a custom-designed polyclonal antibody against an epitope near the C terminus of the Tec1 protein.) The tagged strains were grown under standard biofilm conditions (because the tags do not compromise function, the strains form normal biofilms) and were harvested for chromatin immunoprecipitation. After precipitation using the commercially available Myc antibody or the custom Tec1 antibody, the immunoprecipitated DNA and whole-cell extract were amplified and competitively hybridized to custom whole-genome oligonucleotide tiling microarrays (AMADID #016350) as described in the Extended Experimental Procedures. Display, analysis, and identification of the binding events were determined using MochiView (Homann and Johnson, 2010).

Motif Analysis
Motif analysis was performed using MochiView. MEME was also used to independently verify motifs found by MochiView. See Data S2, Tables S2H–S2M, and the Extended Experimental Procedures for details.

RNA Sequencing of Biofilm and Planktonic Cells
Strand-specific, massively parallel SOLiD System sequencing of RNA from wild-type *C. albicans* biofilm and planktonic cells and mapping of resulting reads were performed as previously described (Tuch et al., 2010). Library amplification and sequencing resulted in 18 million planktonic and 28 million biofilm ~50 nt strand-specific sequence reads mappable to the *C. albicans* genome.

Identification of Novel Transcriptionally Active Regions in Biofilms
nTARs were identified using MochiView. A previously published transcript annotation (Tuch et al., 2010) was used as a starting scaffold, and additional transcribed regions were identified. This approach identified 783 biofilm nTARs distinct from those in the previous annotation (Extended Experimental Procedures and Table S4A).

Differential Expression Analysis of RNA-Seq Data
For every transcribed region in our expanded biofilm genome annotation, mean per nucleotide sequence coverage was extracted from both biofilm and planktonic data sets and transformed into pseudo-RPKM values, and transcripts differentially expressed between the two data sets were determined as described in Extended Experimental Procedures. The union of the RNA-seq and microarray data sets was used to determine the final set of differentially expressed genes (Tables S4B and S4C). Statistical significance (p values) for the association of binding and differential transcription was calculated using a two-tailed Fisher's exact test.

Association of Transcription Regulator Binding Sites with Adjacent Transcripts
To determine the association between transcription regulator binding and differential gene expression, the binding peaks identified by ChIP-chip were mapped to immediately adjacent, divergently transcribed genes. A transcription regulator binding site was considered to be associated with differential expression if at least one divergent flanking transcript was differentially expressed in either the microarray or the RNA-seq comparison.

Exploring Orthology Relationships and Defining Gene Age Categories
Orthologs of the *C. albicans* and *S. cerevisiae* biofilm regulators and their direct targets were identified using freely available orthology mapping programs and by hand annotation using gene trees (See Extended Experimental Procedures). *C. albicans* gene age categories were defined as follows: "old" are members of gene families found in all Ascomycetes, "middle-aged" are members of gene families that arose after the divergence of *Schizosaccharomyces pombe* and *Schizosaccharomyces japonicus* but before the divergence of the CTG clade, and "young" are found only in CTG clade species. Overlap of age categories with biofilm-induced genes is described by the hypergeometric distribution (Extended Experimental Procedures).

ACCESSION NUMBERS

All data have been deposited into the NCBI Gene Expression Omnibus (GEO) portal under the accession numbers GSE21291 (RNA-seq), GSE29785 (ChIP-chip), and GSE30474 (GE Array).

SUPPLEMENTAL INFORMATION

Supplemental Information includes Extended Experimental Procedures, seven figures, seven tables, and two data files and can be found with this article online at doi:10.1016/j.cell.2011.10.048.

ACKNOWLEDGMENTS

REFERENCES

Alabadí, D., Oyama, T., Yanovsky, M.J., Harmon, F.G., Más, P., and Kay, S.A. (2001). Reciprocal regulation between TOC1 and LHY/CCA1 within the Arabidopsis circadian clock. Science 293, 880–883.

Andes, D., Nett, J., Oschel, P., Albrecht, R., Marchillo, K., and Pitula, A. (2004). Development and characterization of an in vivo central venous catheter Candida albicans biofilm model. Infect. Immun. 72, 6023–6031.

Askew, C., Sellam, A., Epp, E., Mallick, J., Hogues, H., Mullick, A., Nantel, A., and Whiteway, M. (2011). The zinc cluster transcription factor Ahr1p directs Mcm1p regulation of Candida albicans adhesion. Mol. Microbiol. 79, 940–953.

Baillie, G.S., and Douglas, L.J. (1999). Role of dimorphism in the development of Candida albicans biofilms. J. Med. Microbiol. 48, 671–679.

Borneman, A.R., Leigh-Bell, J.A., Yu, H., Bertone, P., Gerstein, M., and Snyder, M. (2006). Target hub proteins serve as master regulators of development in yeast. Genes Dev. 20, 435–448.

Bruno, V.M., Wang, Z., Marjani, S.L., Euskirchen, G.M., Martin, J., Sherlock, G., and Snyder, M. (2010). Comprehensive annotation of the transcriptome of the human fungal pathogen Candida albicans using RNA-seq. Genome Res. 20, 1451–1458.

Chandra, J., Kuhn, D.M., Mukherjee, P.K., Hoyer, L.L., McCormick, T., and Ghannoum, M.A. (2001). Biofilm formation by the fungal pathogen Candida albicans: development, architecture, and drug resistance. J. Bacteriol. 183, 5385–5394.

Costerton, J.W., Stewart, P.S., and Greenberg, E.P. (1999). Bacterial biofilms: a common cause of persistent infections. Science 284, 1318–1322.

de Hoon, M.J., Eichenberger, P., and Vitkup, D. (2010). Hierarchical evolution of the bacterial sporulation network. Curr. Biol. 20, R735–R745.

Donlan, R.M., and Costerton, J.W. (2002). Biofilms: survival mechanisms of clinically relevant microorganisms. Clin. Microbiol. Rev. 15, 167–193.

Douglas, L.J. (2003). Candida biofilms and their role in infection. Trends Microbiol. 11, 30–36.

Fernández, A., and Lynch, M. (2011). Non-adaptive origins of interactome complexity. Nature 474, 502–505.

Hamoen, L.W., Venema, G., and Kuipers, O.P. (2003). Controlling competence in Bacillus subtilis: shared use of regulators. Microbiology 149, 9–17.

Harbison, C.T., Gordon, D.B., Lee, T.I., Rinaldi, N.J., Macisaac, K.D., Danford, T.W., Hannett, N.M., Tagne, J.B., Reynolds, D.B., Yoo, J., et al. (2004). Transcriptional regulatory code of a eukaryotic genome. Nature 431, 99–104.

Hawser, S.P., and Douglas, L.J. (1994). Biofilm formation by Candida species on the surface of catheter materials in vitro. Infect. Immun. 62, 915–921.

Hepworth, S.R., Friesen, H., and Segall, J. (1998). NDT80 and the meiotic recombination checkpoint regulate expression of middle sporulation-specific genes in Saccharomyces cerevisiae. Mol. Cell. Biol. 18, 5750–5761.

Homann, O.R., and Johnson, A.D. (2010). MochiView: versatile software for genome browsing and DNA motif analysis. BMC Biol. 8, 49.

Homann, O.R., Dea, J., Noble, S.M., and Johnson, A.D. (2009). A phenotypic profile of the Candida albicans regulatory network. PLoS Genet. 5, e1000783.

Kojic, E.M., and Darouiche, R.O. (2004). Candida infections of medical devices. Clin. Microbiol. Rev. 17, 255–267.

Kolter, R., and Greenberg, E.P. (2006). Microbial sciences: the superficial life of microbes. Nature 441, 300–302.

Lavoie, H., Hogues, H., Mallick, J., Sellam, A., Nantel, A., and Whiteway, M. (2010). Evolutionary tinkering with conserved components of a transcriptional regulatory network. PLoS Biol. 8, e1000329.

Lin, Z., Wu, W.S., Liang, H., Woo, Y., and Li, W.H. (2010). The spatial distribution of cis regulatory elements in yeast promoters and its implications for transcriptional regulation. BMC Genomics 11, 581.

Locke, J.C., Southern, M.M., Kozma-Bognár, L., Hibberd, V., Brown, P.E., Turner, M.S., and Millar, A.J. (2005). Extension of a genetic network model by iterative experimentation and mathematical analysis. Mol. Syst. Biol. 1, 2005.0013.

Long, M., Betrán, E., Thornton, K., and Wang, W. (2003). The origin of new genes: glimpses from the young and old. Nat. Rev. Genet. 4, 865–875.

Losick, R., and Stragier, P. (1992). Crisscross regulation of cell-type-specific gene expression during development in B. subtilis. Nature 355, 601–604.

Madhani, H.D., and Fink, G.R. (1997). Combinatorial control required for the specificity of yeast MAPK signaling. Science 275, 1314–1317.

Mitrovich, Q.M., Tuch, B.B., De La Vega, F.M., Guthrie, C., and Johnson, A.D. (2010). Evolution of yeast noncoding RNAs reveals an alternative mechanism for widespread intron loss. Science 330, 838–841.

Müller, D., and Stelling, J. (2009). Precise regulation of gene expression dynamics favors complex promoter architectures. PLoS Comput. Biol. 5, e1000279.

Nett, J., and Andes, D. (2006). Candida albicans biofilm development, modeling a host-pathogen interaction. Curr. Opin. Microbiol. 9, 340–345.

Nett, J.E., Marchillo, K., Spiegel, C.A., and Andes, D.R. (2010). Development and validation of an in vivo Candida albicans biofilm denture model. Infect. Immun. 78, 3650–3659.

Ni, L., Bruce, C., Hart, C., Leigh-Bell, J., Gelperin, D., Umansky, L., Gerstein, M.B., and Snyder, M. (2009). Dynamic and complex transcription factor binding during an inducible response in yeast. Genes Dev. 23, 1351–1363.

Nobile, C.J., and Mitchell, A.P. (2005). Regulation of cell-surface genes and biofilm formation by the C. albicans transcription factor Bcr1p. Curr. Biol. 15, 1150–1155.

Nobile, C.J., Andes, D.R., Nett, J.E., Smith, F.J., Yue, F., Phan, Q.T., Edwards, J.E., Filler, S.G., and Mitchell, A.P. (2006a). Critical role of Bcr1-dependent adhesins in C. albicans biofilm formation in vitro and in vivo. PLoS Pathog. 2, e63.

Nobile, C.J., Nett, J.E., Andes, D.R., and Mitchell, A.P. (2006b). Function of Candida albicans adhesin Hwp1 in biofilm formation. Eukaryot. Cell 5, 1604–1610.

Nobile, C.J., Schneider, H.A., Nett, J.E., Sheppard, D.C., Filler, S.G., Andes, D.R., and Mitchell, A.P. (2008). Complementary adhesin function in C. albicans biofilm formation. Curr. Biol. 18, 1017–1024.

Nobile, C.J., Nett, J.E., Hernday, A.D., Homann, O.R., Deneault, J.S., Nantel, A., Andes, D.R., Johnson, A.D., and Mitchell, A.P. (2009). Biofilm matrix regulation by Candida albicans Zap1. PLoS Biol. 7, e1000133.

Ramage, G., VandeWalle, K., López-Ribot, J.L., and Wickes, B.L. (2002). The filamentation pathway controlled by the Efg1 regulator protein is required for normal biofilm formation and development in Candida albicans. FEMS Microbiol. Lett. 214, 95–100.

Ramage, G., Tomsett, K., Wickes, B.L., López-Ribot, J.L., and Redding, S.W. (2004). Denture stomatitis: a role for Candida biofilms. Oral Surg. Oral Med. Oral Pathol. Oral Radiol. Endod. 98, 53–59.

Sahni, N., Yi, S., Daniels, K.J., Huang, G., Srikantha, T., and Soll, D.R. (2010). Tec1 mediates the pheromone response of the white phenotype of Candida

albicans: insights into the evolution of new signal transduction pathways. PLoS Biol. *8*, e1000363.

Schinabeck, M.K., Long, L.A., Hossain, M.A., Chandra, J., Mukherjee, P.K., Mohamed, S., and Ghannoum, M.A. (2004). Rabbit model of Candida albicans biofilm infection: liposomal amphotericin B antifungal lock therapy. Antimicrob. Agents Chemother. *48*, 1727–1732.

Sellam, A., Tebbji, F., and Nantel, A. (2009). Role of Ndt80p in sterol metabolism regulation and azole resistance in Candida albicans. Eukaryot. Cell *8*, 1174–1183.

Sellam, A., Hogues, H., Askew, C., Tebbji, F., van Het Hoog, M., Lavoie, H., Kumamoto, C.A., Whiteway, M., and Nantel, A. (2010). Experimental annotation of the human pathogen Candida albicans coding and noncoding transcribed regions using high-resolution tiling arrays. Genome Biol. *11*, R71.

Süel, G.M., Garcia-Ojalvo, J., Liberman, L.M., and Elowitz, M.B. (2006). An excitable gene regulatory circuit induces transient cellular differentiation. Nature *440*, 545–550.

Sugino, R.P., and Innan, H. (2011). Natural selection on gene order in the genome re-organization process after whole genome duplication of yeast. Mol. Biol. Evol. Published online May 5, 2011. 10.1093/molbev/msr118.

Tuch, B.B., Mitrovich, Q.M., Homann, O.R., Hernday, A.D., Monighetti, C.K., De La Vega, F.M., and Johnson, A.D. (2010). The transcriptomes of two heritable cell types illuminate the circuit governing their differentiation. PLoS Genet. *6*, e1001070.

Uppuluri, P., Chaturvedi, A.K., Srinivasan, A., Banerjee, M., Ramasubramaniam, A.K., Köhler, J.R., Kadosh, D., and Lopez-Ribot, J.L. (2010a). Dispersion as an important step in the Candida albicans biofilm developmental cycle. PLoS Pathog. *6*, e1000828.

Uppuluri, P., Pierce, C.G., Thomas, D.P., Bubeck, S.S., Saville, S.P., and Lopez-Ribot, J.L. (2010b). The transcriptional regulator Nrg1p controls Candida albicans biofilm formation and dispersion. Eukaryot. Cell *9*, 1531–1537.

Wapinski, I., Pfeffer, A., Friedman, N., and Regev, A. (2007). Natural history and evolutionary principles of gene duplication in fungi. Nature *449*, 54–61.

Webb, B.C., Thomas, C.J., Willcox, M.D., Harty, D.W., and Knox, K.W. (1998). Candida-associated denture stomatitis. Aetiology and management: a review. Part 2. Oral diseases caused by Candida species. Aust. Dent. J. *43*, 160–166.

Wilson, J. (1998). The aetiology, diagnosis and management of denture stomatitis. Br. Dent. J. *185*, 380–384.

Wilson, N.K., Foster, S.D., Wang, X., Knezevic, K., Schütte, J., Kaimakis, P., Chilarska, P.M., Kinston, S., Ouwehand, W.H., Dzierzak, E., et al. (2010). Combinatorial transcriptional control in blood stem/progenitor cells: genome-wide analysis of ten major transcriptional regulators. Cell Stem Cell *7*, 532–544.

Young, R.A. (2011). Control of the embryonic stem cell state. Cell *144*, 940–954.

Zhu, C., Byers, K.J., McCord, R.P., Shi, Z., Berger, M.F., Newburger, D.E., Saulrieta, K., Smith, Z., Shah, M.V., Radhakrishnan, M., et al. (2009). High-resolution DNA-binding specificity analysis of yeast transcription factors. Genome Res. *19*, 556–566.